ACS Sustainable Chemistry & Engineering

Research Article

Cite This: ACS Sustainable Chem. Eng. 2019, 7, 2216−2224

pubs.acs.org/journal/ascecg

Cross-Linked Acrylic Polymers from the Aqueous Phase of Biomass Pyrolysis Oil and Acrylated Epoxidized Soybean Oil

Mehul Barde,[†,‡] Katrina Avery,[†,‡] Charles W. Edmunds,[§] Nicole Labbé,[§] and Maria L. Auad*[,∥,†,‡]

[†]212 Ross Hall, Department of Chemical Engineering, Auburn University, Auburn, Alabama 36849, United States of America

[‡]Center for Polymers and Advanced Composites, Auburn University, Auburn, Alabama 36849, United States of America

[§]2506 Jacob Drive, Center for Renewable Carbon, University of Tennessee, Knoxville, Tennessee 37996, United States of America

Supporting Information

ABSTRACT: Development of cross-linked, soft polymeric materials from biomass has been a focus of research. The aqueous phase of biomass pyrolysis oil (bio-oil) has been used as a precursor for monomer synthesis. Pine wood was ground and pyrolyzed to produce liquid bio-oil which was further separated into organic and aqueous phases. Gas chromatography−mass spectroscopy (GC-MS), ^{31}P-nuclear magnetic resonance (^{31}P NMR), ^{1}H NMR, and Fourier transform-infrared (FTIR) spectroscopy were used for the characterization of bio-oil and its derivatives. Methacrylation reaction was carried out on the concentrated aqueous phase to yield methacrylated aqueous bio-oil. Acrylated epoxidized soybean oil (AESO) and methacrylated aqueous bio-oil were blended in different proportions and were polymerized by free radical polymerization. The polymer samples were evaluated by FTIR, dynamic mechanical analysis (DMA), Soxhlet extraction, and scanning electron microscopy (SEM). Tensile modulus, storage modulus, active chains density, and mass retention increased with higher AESO content. The polymers displayed sub-ambient glass transition temperatures (−30 to −21 °C). The impact of plasticizing and cross-linking effects of polymer chains on the glass transition temperature was studied with the theoretical Fox and Loshaek models. Utilization of the low-valued aqueous bio-oil and soybean oil renders the cross-linked polymers potential replacement of conventional polymers and helps to improve the overall sustainability.

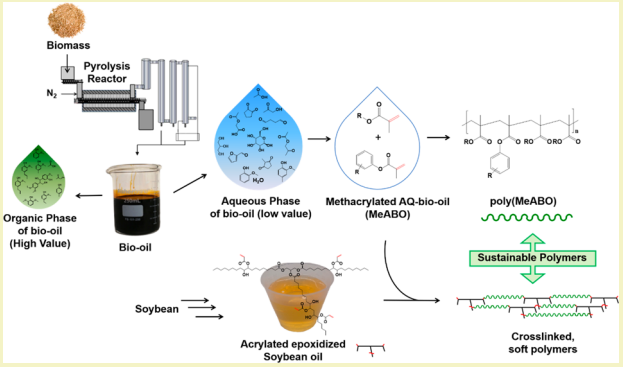

KEYWORDS: *Lignocellulosic biomass, Aqueous bio-oil, Methacrylates, Acrylated epoxidized soybean oil, Cross-linked polyacrylate*

INTRODUCTION

Plant biomass has been widely accepted as an alternate and renewable resource of chemicals and fuels. Depending on the species, plant biomass can be remarkably different in its components and is characterized by great complexity at the molecular level. Lignocellulosic biomass is one of the main plant biomass types and is comprised of lignin, cellulose, and hemicellulose biopolymers bound together.[1] The breakdown of complex macromolecules in the biomass to smaller compounds has been a general approach to obtain chemicals. This can be achieved by employing various chemical, thermochemical, and biochemical processes, such as gasification, pyrolysis,[2,3] liquefaction,[4,5] torrefaction, and fermentation. Biomass can be subjected to a fast pyrolysis process to efficiently produce high yields of the liquid fraction that is often called biomass pyrolysis oil or bio-oil.[6] The fast pyrolysis process often yields bio-oil liquids into separated phases, i.e., a useful, organic-rich phase and an aqueous phase which is mostly regarded as a waste stream.[7] The aqueous phase of bio-oil can have a water content as high as 80%, with the remaining liquid appearing as polar organic compounds which are degradation products of cellulose and hemicellulose.[8,9] Since the aqueous phase generally has a high water content, it is rendered as useless for use as conventional fuel. Upgrading the aqueous phase to a liquid fraction with a higher heating value can be technically, as well as economically, cumbersome. Several attempts have been documented regarding the utilization of the aqueous phase of bio-oil for producing hydrogen by steam reforming[10−16] and supercritical water reforming.[17] Nevertheless, the bio-oil aqueous phase has not been successfully used for producing functional chemicals, monomers and polymers, which are highly value-added applications. On the other hand, the bio-oil organic phase has been extensively used for synthesis of monomers and polymers such as phenol-formaldehyde,[18,19] epoxy,[20−22] polyurethane,[23,24] etc.

In the current study, we focus on utilization of waste aqueous bio-oil to develop acrylic polymers. Conventionally,

Received: September 24, 2018
Revised: December 18, 2018
Published: December 19, 2018

DOI: 10.1021/acssuschemeng.8b04897
ACS Sustainable Chem. Eng. 2019, 7, 2216−2224

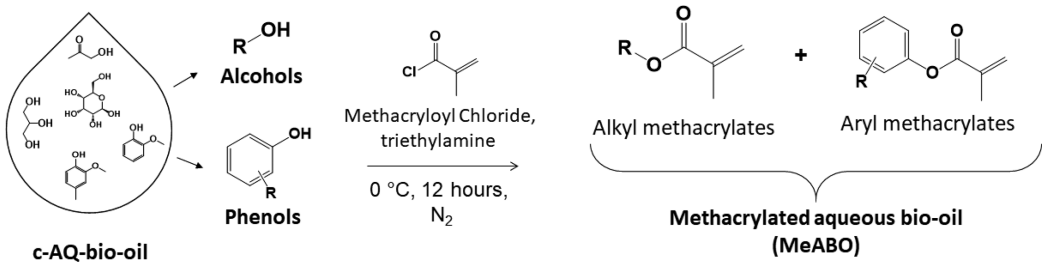

Figure 1. Methacrylation of c-AQ-bio-oil.

the most commonly used acrylic polymers are obtained from acrylate and/or methacrylate monomers, such as methyl methacrylate, ethyl acrylate, *n*-butyl acrylate, etc. Polyacrylates are used in many applications, including coatings,[25−27] adhesives,[28,29] composites,[30−32] superabsorbent materials,[33,34] etc. Typical acrylate and methacrylate monomers are alkyl esters of acrylic acid and methacrylic acid, respectively, which are derived from petrochemicals. Acrylic monomers have been synthesized from a few biomass resources in the past, such as soybean oil,[35] vanillin,[36] lignin,[37] etc. Acrylated epoxidized soybean oil (AESO) has been successfully used for copolymerization in several studies. The approach of this study is to exploit aliphatic hydroxyl compounds available in the aqueous bio-oil to produce methacrylate monomers and subsequent polymers. We have also employed AESO in varying proportions to develop cross-linked polymers with improved thermo-mechanical properties.

EXPERIMENTAL SECTION

Materials. Acetone (≥99.5% ACS), benzoyl peroxide (97%) (dry weight) wetted with ca. 25% water, chloroform (≥99.8% stabilized ACS), chromium(III) acetylacetonate (≥98.0%) (by titrimetric analysis), chloroform-[D_1] (≥99.8% (isotopic) with TMS (0.03 vol %) stabilized, MagniSolv for NMR spectroscopy, dichloromethane (≥99.5% stabilized ACS), *N*-hydroxy-5-norbornene-2,3-dicarboximide (≥97%) (NHND), methacryloyl chloride (97%), and triethylamine (99%) were ordered from VWR International, USA. 2-Chloro-4,4,5,5-tetramethyl-1,3,2-dioxaphospholane (97%) (TMDP) and acrylated epoxidized soybean oil (contains 4000 ppm monomethyl ether hydroquinone as an inhibitor) were purchased from Sigma-Aldrich, USA. The aqueous phase of bio-oil was obtained from pine wood as per the procedure described in the Methods.

Methods. *Fast Pyrolysis of Pine.* Clean pine wood with particles less than 4 mm in size were fed into an auger-fed pyrolysis reactor at 7.3 kg/h and with the reactor temperature raised to 500 °C and N_2 purge flow rate at 50 L/min. A detailed instrument description was reported previously.[38] Product vapors of pyrolyzed biomass were condensed to yield a liquid bio-oil which was further separated into two phases, namely, an aqueous phase (AQ-bio-oil) and an organic phase (ORG-bio-oil). The yields of bio-oil and biochar were measured gravimetrically, and the yield of noncondensable gases was calculated by difference. The bio-oil samples were stored in the freezer at −10 °C. AQ-bio-oil was heated at 80 °C for 15 min under reduced pressure using a rotary evaporator to concentrate the bio-oil phase. The concentrated AQ (c-AQ-bio-oil) was characterized and used for chemical modification.

Characterization of AQ-Bio-oil. GC-MS was used to measure the chemical composition of the produced AQ-bio-oil. The AQ-bio-oil was dissolved in 99.9% pure MeOH (1 mL of bio-oil in 9 mL of MeOH) and filtered with a PTFE syringe filter (0.20 μm), and a 1 μL aliquot was injected into the GC-MS system (Clarus 680 gas chromatograph and Clarus SQ 8C mass spectrometer, PerkinElmer, USA). The injection was performed at a split ratio of 80:1 and an injector temperature of 270 °C. An Elite 1701 MS capillary column (60 m × 0.25 mm ID by 0.25 μm film thickness) with a carrier gas (ultrahigh-purity helium, 99.9999%) flow rate of 1 cm^3/min and pressure of 17.3 psi were used. The GC furnace was initially held at 50 °C for 4 min, was ramped to 280 °C at 5 °C/min, and then held at 280 °C for 5 min. The MS was held at 270 °C with an ionization energy of 70 eV. Chromatogram peaks were extracted using TubroMass GC-MS software, and peaks were identified with the National Institute of Standards and Technology (NIST) library.

The water content of the bio-oils was measured by Karl Fischer titration (Metrohm 787 KF Titrino) following the American Society for Testing and Materials protocol ASTM D4377-00.[39] The pH of the bio-oil samples was measured using a pH meter after stirring 1 mL of bio-oil into 50 mL of DI water. The total acid number (TAN) was measured by dissolving 0.5 g of bio-oil in 25 mL of 1:1 isopropyl alcohol/water then titrating the mixture with 0.1 N KOH to a pH of 11 in accordance with ASTM D664-11a.[40] The density of the bio-oil samples was determined using a 2 mL glass pycnometer according to ASTM D1475-13.[41] Analyses were performed in duplicate. Viscosity measurements were performed using TA Instruments AR-G2 (U.S.) instrumentation using a 40 mm parallel plate geometry. The measured viscosity of the AQ-bio-oil was 0.012 ± 0.006 Pa·S at 1 s^{-1} and 25 °C.

For ^{31}P NMR spectroscopy, the bio-oil phases were phosphorylated as per the procedure mentioned in the literature.[42] NHND and chromium(III) acetylacetonate (20 mg each) were dissolved in the mixture of 3 mL of pyridine and 2 mL of deuterated chloroform to prepare the stock solution. Then, 550 μL of stock solution was added to around 20 mg of the desired bio-oil sample, and the mixture was stirred well. TMDP (150 μL) was then added to the mixture, and the mixture was stirred well to make the solution homogeneous. The prepared solution was then transferred to the NMR spectroscopy tube, and the spectrum was acquired with a Bruker Avance II 250 MHz spectrometer using an inverse-gated decoupling pulse sequence, 90-degree pulse angle, 25 s pulse delay, and 128 scans. The hydroxyl content of the bio-oil phases was calculated by integrating relevant peaks compared to the internal standard NHND.

Fourier transform infrared spectroscopy was performed on bio-oil samples and synthesized products using a Thermo Scientific Nicolet 6700 FT-IR spectrophotometer equipped with attenuated total reflection (ATR) and OMNIC 7.3 software. IR spectra were collected in the wavenumber range of 400 to 4000 cm^{-1} at a resolution of 4 cm^{-1} and 64 scans.

Synthesis and Characterization of Methacrylated Aqueous Bio-oil (MeABO). The methacrylation procedure was adapted from literature[43] and used with modifications. Around 38 g of c-AQ-bio-oil was dissolved in 150 mL of acetone in a jacketed, glass reactor equipped with a mechanical stirrer. Triethylamine (1.2 equiv/OH) was added to the reactor with stirring. Water−methanol coolant was circulated through the jacket to reduce the temperature of the reaction mixture to 0 °C. Methacryloyl chloride (1.2 equiv/OH) dissolved in acetone was added dropwise to the reaction mixture over 30 min. After the addition was completed, the mixture was stirred for 6 h and the cooling was turned off. The reaction product was heated at 40 °C under reduced pressure to remove acetone and was further mixed in chloroform. The chloroform phase was washed with water to remove salts. Chloroform was removed via distillation using a rotary evaporator, and the product, named as methacrylated aqueous bio-oil (MeABO), was characterized by FTIR spectroscopy, ^{1}H NMR spectroscopy, and ^{31}P NMR spectroscopy. ^{1}H NMR spectra were

DOI: 10.1021/acssuschemeng.8b04897
ACS Sustainable Chem. Eng. 2019, 7, 2216−2224

collected with a Bruker Avance II 600 MHz spectrometer using 64 scans. Deuterated chloroform was used as the solvent with tetramethylsilane added as the reference.

AQ-bio-oil was first concentrated by removing water at reduced pressure and then was functionalized by incorporating methacrylate groups. Since AQ-bio-oil is originally dilute in nature, it is characterized by peaks with lower intensities. Further, the removal of other volatile organic compounds during rotary evaporation can lead to the absence of a few peaks that might have been otherwise displayed. In the case of MeABO, the purification was performed. Nonetheless, the presence of traces of byproducts and non-participating compounds might have an impact of additional peaks appearing in the spectra.

The measured viscosity of the MeABO was 2.18 ± 0.27 Pa·S at 1 s^{-1} and 25 °C. In addition, the viscosity of the AESO was 25.7 ± 2.1 Pa·S at the same conditions.

Figure 1 depicts methacrylation of AQ-bio-oil and further polymerization. Theoretically, it is expected to obtain a mixture of chemically similar compounds predominantly appearing as alkyl methacrylates and aryl methacrylates.

Polymerization of Methacrylated Monomers with AESO. MeABO and AESO were mixed in the proportions explained in Table 1. Initiator benzoyl peroxide was ground and added (3 wt %) to each monomer blend. All monomer blends were poured into a Teflon cavity mold and heated at 40 °C in a conventional oven and vacuum oven for 1 day each to remove any residual solvent. The samples were heated at 70 °C for 12 h, 90 °C for 6 h, and 120 °C for 6 h under vacuum. After the heating program, the samples were allowed to cool and then were taken for further characterization and analysis. The typical reactions and structures of polymeric systems are described in Figures S1, S2 and S3 of the Supporting Information. Due to a range of possible, different monomers, it is expected to have a random structure for poly(MeABO) and its cross-linked systems with AESO.

Table 1. Preparation of MeABO/AESO Blends

sample name	amount of MeABO in the sample	amount of AESO in the sample	samples after polymerization
MeABO	100%	0%	poly(MeABO)
75:25A	75%	25%	poly(75:25A)
50:50A	50%	50%	poly(50:50A)
25:75A	25%	75%	poly(25:75A)
AESO	0%	100%	poly(AESO)

Soxhlet Extraction. The polymer samples were subjected to Soxhlet extraction by refluxing 200 mL of dichloromethane for 24 h using a Soxhlet extraction apparatus. After the extraction, the insoluble solids were dried, and the mass retained for each polymeric system was reported as the percent of the initial sample weight.

Dynamic Mechanical Analysis. Thermo-mechanical evaluation of polymer samples was performed using a TA Instruments dynamic mechanical analyzer RSAIII. Cyclic stress was applied at a 1 Hz frequency on the horizontal specimen using three-point bending geometry to yield a constant 0.1% strain (specimen: 35 mm × 5 mm × 2 mm). The temperature was increased from −100 to 100 °C at 5 °C/min. The glass transition temperature, storage modulus, and active chains density were reported. The glass transition temperature was considered at the intersection of tangents (in the glassy region and glass-transition region) to the storage modulus versus the temperature curve.

RESULTS AND DISCUSSION

Characterization of AQ-Bio-oil. Pyrolysis process results and the properties of AQ-bio-oil are listed in Table 2.

GC-MS analysis of AQ-bio-oil (depicted in Figure 2) revealed the major peaks corresponding to the aliphatic compounds. Most of the detected aliphatic compounds can be classified into alcohols, carboxylic acids, aldehydes, ketones, and sugars. Substituted phenols and furans were also detected in AQ-bio-oil.

Table 2. Properties of AQ-Bio-oil

Fast Pyrolysis of Pine	
bio-oil yield (%)	53.7 ± 0.0
biochar yield (%)	30.4 ± 0.0
noncondensable gas yield (%)	15.9 ± 0.0
AQ-Bio-oil	
water content (%)	49.0 ± 2.6
total acid number (mg KOH/g bio-oil)	131.3 ± 1.4
density (g/mL)	1.12 ± 0.00
pH	2.7 ± 0.0

^{31}P NMR spectroscopy yielded quantification of hydroxyl number, which was in agreement with GC-MS results. The amount of aliphatic OH was observed to be the maximum among all kinds of OH groups. After the AQ-bio-oil was concentrated by rotary evaporation, it was observed that all organic hydroxyl groups showed a higher amount per gram of bio-oil, as shown in Figure 3. This is due to the removal of a significant amount of water from the AQ-bio-oil.

Characterization of MeABO. In the FTIR spectrum of MeABO in Figure 4 (b), a peak was observed at 1677 cm^{-1} which was due to the stretching vibration of C═C incorporated by the methacrylation reaction. A weak stretching vibration of sp^2═C—H was also observed near 2983 cm^{-1}. Another important observation was the reduction of the broad peak at 3383 cm^{-1} related to the O—H stretch. Other peaks present in Figure 4 (b) can be assigned to their respective groups: 2928 cm^{-1} for sp^3 C—H, 1722 cm^{-1} for C═O, 1150 cm^{-1} for C—O bonded to a carbonyl group, and 1031 cm^{-1} for C—O on the alcohol side of the ester group.

In Figure 5 (a), the ^{1}H NMR spectrum of MeABO reflected the appearance of peaks at 5.51 and 6.08 ppm due to the protons deshielded by the C═C group. Protons on the —CH_3 group adjacent to the C═C also caused the appearance of a peak at 1.94 ppm.

Both FTIR and ^{1}H NMR spectroscopy confirmed the presence of olefin functionality in the synthesized methacrylated phase. Quantification of hydroxyl groups by ^{31}P NMR spectroscopy before and after the modification of AQ-bio-oil is presented in Table 3. Methacrylation of c-AQ-bio-oil consumed the most aliphatic OH and all phenolic OH groups. The presence of a higher acidic OH value can be attributed to the conversion of methacryloyl chloride to methacrylic acid, which is also a methacrylic monomer.

FTIR Spectroscopy of Polymers. As shown in Figure 6 (a), FTIR spectroscopy of all monomer blends confirmed the presence of a C═C peak at 1677 cm^{-1} coming from MeABO and at 1633 cm^{-1} coming from AESO. After polymerization (Figure 6 (b)), the peaks corresponding to the C═C disappeared, indicating the reaction of C═C functionalities by free radicals formed by thermal, homolytic cleavage of the peroxide group of the benzoyl peroxide initiator. The FTIR spectroscopy proved the exploitation of olefins to carry out the polymerization.

Soxhlet Extraction. The mass retained after performing the Soxhlet extraction with dichloromethane for 24 h was observed to increase by raising the amount of AESO. (Table 4). A greater amount of AESO produces denser networks which resist the solubilization by dichloromethane. For poly(AESO), the highest mass retention was observed with a

DOI: 10.1021/acssuschemeng.8b04897
ACS Sustainable Chem. Eng. 2019, 7, 2216−2224

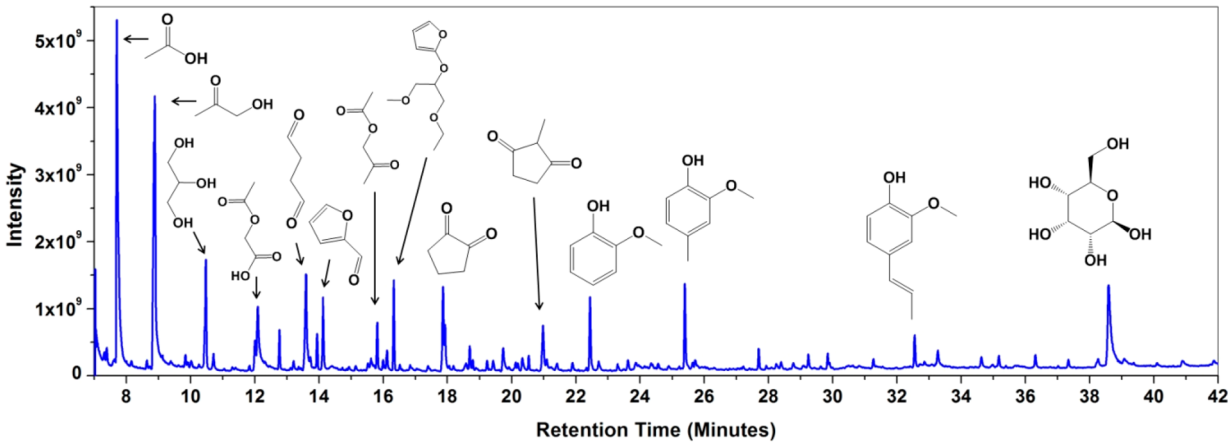

Figure 2. GC-MS analysis of AQ-bio-oil.

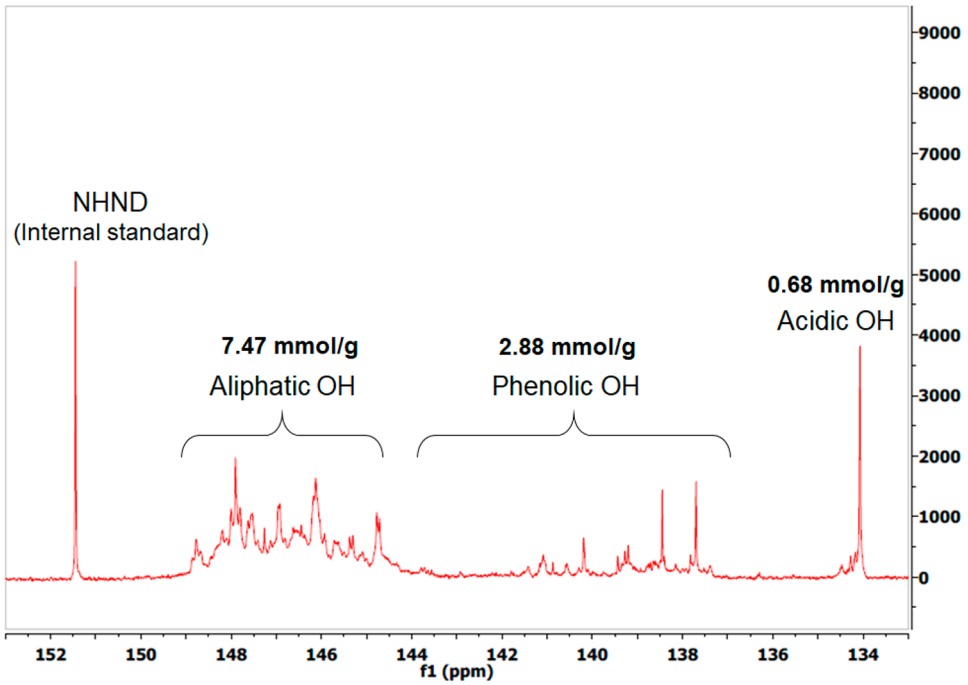

Figure 3. ^{31}P NMR spectra of c-AQ-bio-oil.

very small amount being solubilized. The AESO has a bulky structure, and it can offer steric hindrance due to long aliphatic chains. So, the increase in the amount of AESO increases the possibility of steric hindrance as much as the cross-linking. We studied the effects of these competing phenomena on the glass transition temperature (see section below) of the systems and observed that the enhancement of glass transition temperature by increasing cross-linking has been compensated by the plasticization of long aliphatic chains.

The higher amount of AESO offers a greater number of cross-links for reacting with MeABO as well as AESO, and it is expected to have increased mass retention after Soxhlet extraction with an increasing amount of AESO.

Dynamic Mechanical Analysis of Polymers. Dynamic analysis with three-point bending revealed the change in storage modulus (real component of the modulus relating to the elastic nature), loss modulus (complex component of the modulus relating to the viscous nature), and tan δ (ratio of loss to storage modulus) with respect to the temperature. Storage moduli at ambient conditions (at 25 °C) and in the rubbery plateau (at 80 °C) and the glass transition temperature (considered at the maximum of tan δ) are reported in Table 4. For poly(MeABO), the rubbery plateau was not observed after a sharp decline in storage modulus. Poly(MeABO) does not have AESO cross-links and is expected to behave more like a linear, random copolymer. The storage moduli of cross-linked samples increased with increasing AESO content, and this phenomenon can be explained by the higher cross-link density of the network. The active chains density (n) of all the samples was calculated by the following equation:

$$n = \frac{E'}{3RT} \quad (1)$$

where E' is the storage modulus from the rubbery plateau (at 80 °C), T the temperature at which the corresponding value of the modulus is taken, and R is the universal gas constant. All quantities bear SI units. The increase in the value of active chains density with the increase in AESO content was due to

DOI: 10.1021/acssuschemeng.8b04897
ACS Sustainable Chem. Eng. 2019, 7, 2216−2224

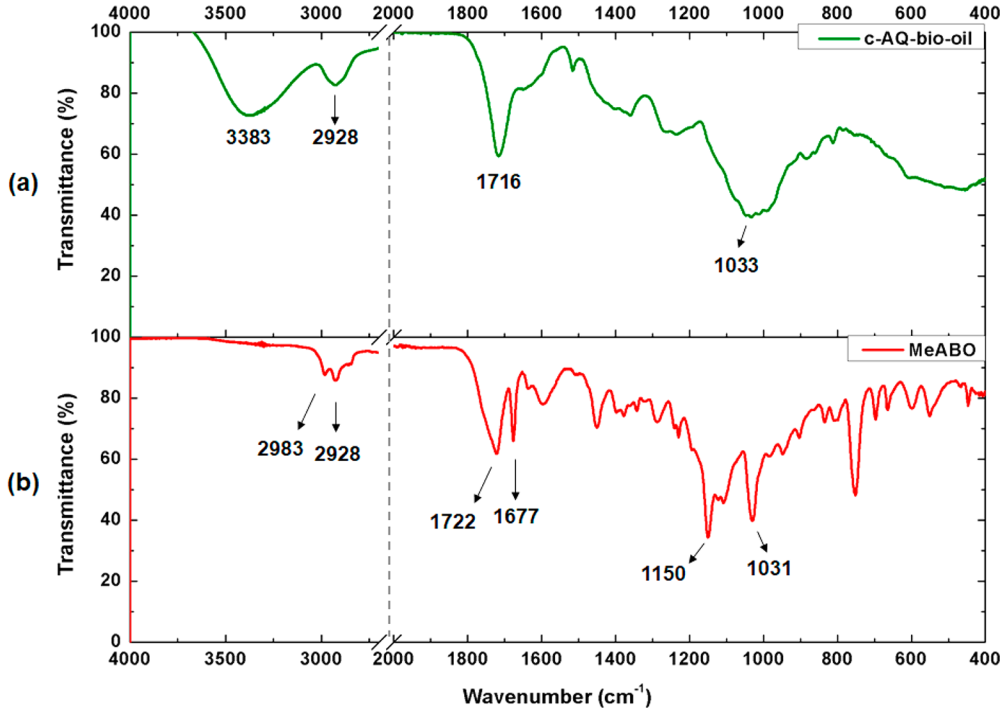

Figure 4. FTIR spectra of (a) c-AQ-bio-oil and (b) MeABO (note: all numbers are in cm^{-1}).

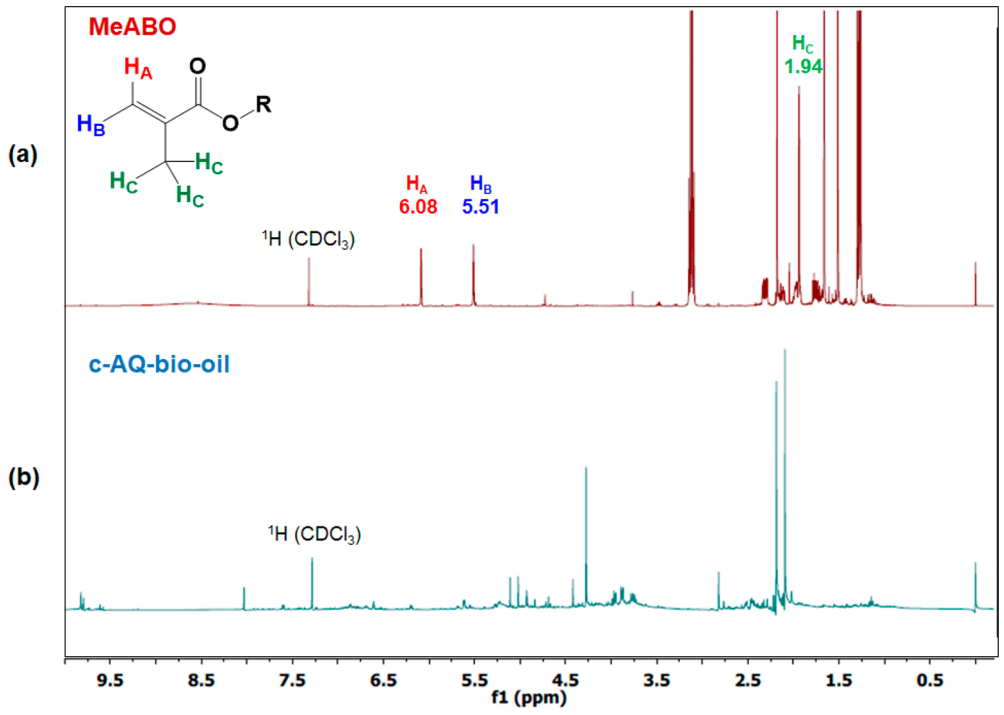

Figure 5. ^{1}H NMR spectra of (a) MeABO and (b) c-AQ-bio-oil (note: all numbers are in ppm).

the multiacrylate functionality of AESO. The plots of storage modulus and tan δ against temperature are provided in Figure 7

Two major phenomena affecting glass transition temperature can be considered for the cross-linked polymers presented in the current study, namely, effect of cross-linking by multifunctional acrylates and effect of long, linear aliphatic chains of AESO. The longer the alkyl chain of the acrylate monomer is, the higher is the plasticizing effect, which results in more decline in the glass transition temperature of the polymer.[44] The same effect was observed in the case of polymethacrylates too.[44,45] As AESO quantity is increased, long aliphatic chains of AESO occupy more volume and space out the polymer chains, imparting a plasticizing effect. Thus, increasing the amount of cross-linkable, multifunctional acrylate with a long, aliphatic structure can enhance the modulus by cross-linking but reduce the glass transition temperature due to the competing, plasticizing effect. Similar

DOI: 10.1021/acssuschemeng.8b04897
ACS Sustainable Chem. Eng. 2019, 7, 2216−2224

Table 3. ^{31}P-NMR Spectroscopy of AQ-Bio-oil, c-AQ-Bio-oil, and MeABO

OH type			range (ppm)	AQ-bio-oil	c-AQ-bio-oil	MeABO
aliphatic OH			150−145.5	3.95	7.47	0.26
phenolic OH	C-5 substituted condensed phenolic OH	*β*-5	144.7−142.8	0.01	0.70	0
		4-O-5	142.8−141.7	0	0.11	0
		5-5	141.7−140.2	0.14	0.48	0
	guaiacyl phenolic OH		140.2−139.0	0.04	0.54	0
	catechol type OH		139.0−138.2	0.13	0.52	0
	p-hydroxyphenyl OH		138.2−137.3	0.06	0.54	0
acidic OH			136.6−133.6	0.34	0.68	1.58
total				4.67	11.04	1.84

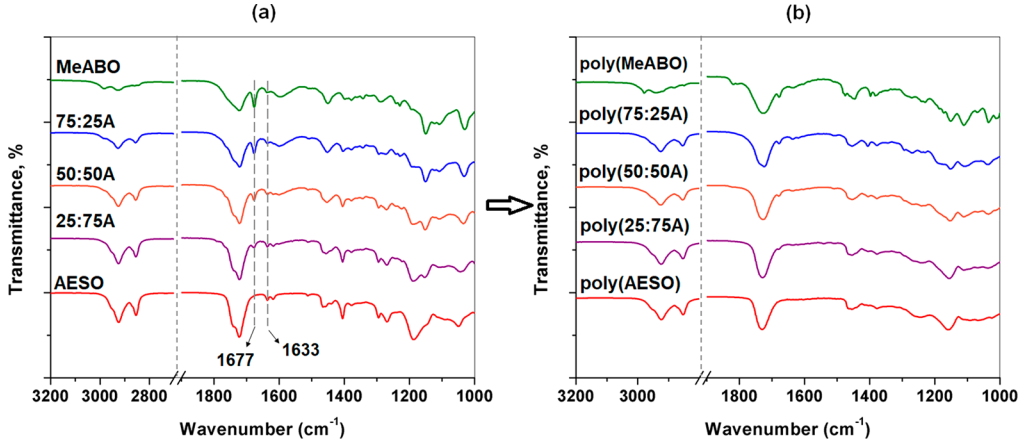

Figure 6. FTIR spectroscopy of (a) monomer blends of MeABO and AESO and (b) polymeric systems of MeABO and AESO.

Table 4. Thermo-Mechanical Properties of Crosslinked Polyacrylate Samples

	glass transition temperature, T_g (°C)		storage modulus, E' (MPa)			
polymer sample	at maximum in tan δ	at intersection of tangents to storage modulus (onset T_g)	at 25 °C	at 80 °C	active chains density, n (mol/m^3)	mass retention (%) by Soxhlet extraction
poly(MeABO)	10.2 ± 5.7	−29.6 ± 0.0	14.3	N/A	N/A	45
poly(75:25A)	16.7 ± 0.8	−21.4 ± 1.4	59.0	5.9	670	61
poly(50:50A)	15.7 ± 0.9	−24.2 ± 2.0	53.0	17.7	2007	72
poly(25:75A)	10.0 ± 0.9	−24.4 ± 2.1	61.8	21.2	2409	86
poly(AESO)	12.2 ± 4.7	−25.5 ± 1.9	113.3	38.7	4380	93

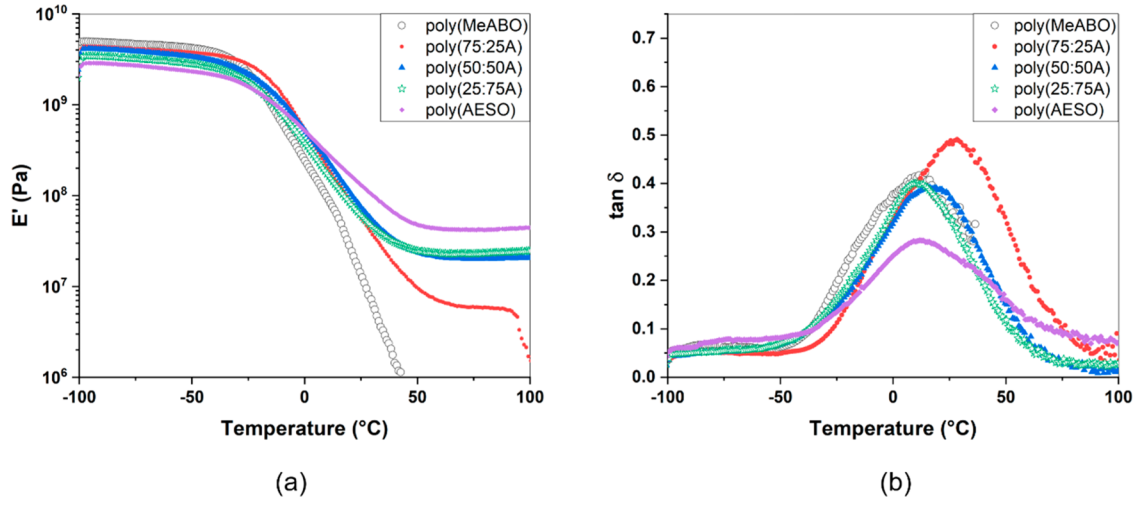

Figure 7. Dynamic mechanical analysis of cross-linked acrylates: (a) storage modulus and (b) tan δ.

DOI: 10.1021/acssuschemeng.8b04897
ACS Sustainable Chem. Eng. 2019, 7, 2216−2224

observations have been reported in other studies which utilized AESO,[35,36,46] soy protein,[47] PEGDMA,[48] etc., in the development of polyacrylates. A thorough analysis of the varying effects on the glass transition temperature has been carried out in the case of cross-linking and copolymerization of methyl methacrylate and glycol dimethacrylates.[49,50]

In the present study, the effect of copolymerization has been assessed by using the Fox equation. Onset T_g data have been taken into consideration for better accuracy. As discussed earlier, poly(MeABO) resembles a linear copolymer structurally, but poly(AESO) is a cross-linked system. The plasticizing effect of poly(AESO) on glass transition temperature was predicted by estimating the theoretical glass transition temperature of linearly homopolymerized AESO using the group contribution scheme proposed as per the following equation.[51]

$$T_{g_{poly}} = \frac{1}{\sum (M_i + M_j)} \left[\sum_{i=1}^{n} (T_{gi} M_i) + \sum_{j=1}^{m} (T_{gj} M_j) \right] \quad (2)$$

where Tg_i and M_i are the glass transition temperature and molecular weight of the groups in the main chain, respectively, whereas Tg_j and M_j are the glass transition temperature and molecular weight of the groups in the side chain of the polymer structure, respectively. The effect of the cross-linking contribution has been analyzed with the help of the Fox and Loshaek model.[52,53]

$$T_{gTotal} = T_{gFox} + \frac{K}{M_c} \quad (3)$$

where the K/M_c factor represents the cross-linking effect. M_c is the molecular weight of fragments between the cross-linking points and was calculated with the help of experimental values of the density of the sample and active chains density. The total effect of the two effects was studied and compared with the experimental values. The value of K was taken as 5200 K g/mol.[52,54] The total effect of cross-linking and plasticizing segments is denoted in Figure 8 and was found to be closer to experimental values.

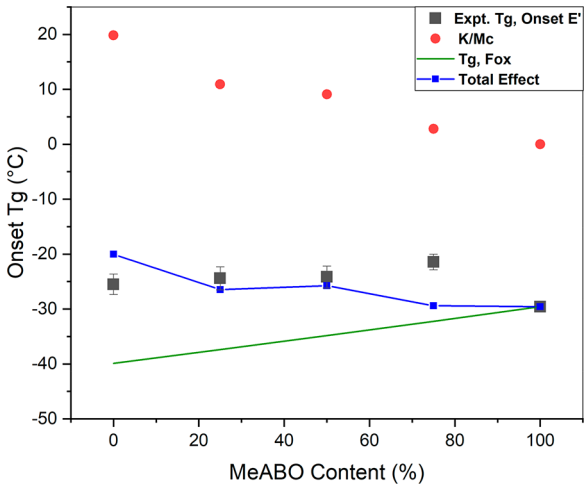

Figure 8. Glass transition temperature of cross-linked acrylates and effects of copolymerization and cross-linking.

CONCLUSIONS

The aqueous phase of bio-oil contains modifiable hydroxyl compounds which can be transformed into methacrylic monomers by the methacrylation reaction. The methacrylated aqueous bio-oil is a mixture of methacrylic monomers synthesized from corresponding alcohols and phenols present in the aqueous bio-oil. Free radical polymerization of methacrylated aqueous bio-oil is possible and yields a predominantly non-cross-linked copolymer. The mechanical properties of methacrylated bio-oil are improved by cross-linking with acrylated epoxidized soybean oil; however, the glass transition temperature is reduced due to the plasticizing effect of long, aliphatic chains of the fatty acid portion present in acrylated epoxidized soybean oil. The effect of cross-link density of polymeric samples is evident from the measured values of tensile modulus, storage modulus, active chains density, and mass retention by Soxhlet extraction. The experimental values of glass transition temperature (onset T_g values) can be fitted with the help of the Fox and Loshaek model. Morphological characteristics are similar in the case of all polymeric samples, with differences appearing in the brittle fracture in the case of cross-linked polymers. Utilization of aqueous bio-oil and soybean oil, both of which are biomass-derived, tend to enhance sustainability of the cross-linked polymers, which can be used in the applications of elastomers, packaging materials, and composites.

ASSOCIATED CONTENT

Supporting Information

The Supporting Information is available free of charge on the ACS Publications website at DOI: 10.1021/acssuschemeng.8b04897.

Polymerization of MeABO (Figure S1), polymerization of AESO (Figure S2), and polymerization of MeABO and AESO (Figure S3) (PDF)

AUTHOR INFORMATION

Corresponding Author

*E-mail: auad@auburn.edu. Tel.: +1-334-844-5459.

ORCID

Charles W. Edmunds: 0000-0002-2356-7312
Nicole Labbé: 0000-0002-2117-4259
Maria L. Auad: 0000-0001-6932-5645

Present Address

‖Dr. Maria L. Auad, 320 Ross Hall, Department of Chemical Engineering, Auburn University, Auburn, AL 36849, United States of America.

Notes

The authors declare no competing financial interest.

ACKNOWLEDGMENTS

The authors would like to acknowledge the U.S. Department of Agriculture, National Institute of Food and Agriculture (USDA-NIFA-2015-67021-22842), the NSF-CREST Center of Excellence in Nano-Bio Materials derived from biorenewable and waste resources, and the NSF-CREST Center for Sustainable Lightweight Materials (C-SLAM) (award no. 1735971) for funding this study.

DOI: 10.1021/acssuschemeng.8b04897
ACS Sustainable Chem. Eng. 2019, 7, 2216−2224

REFERENCES

(1) Terashima, N.; Kitano, K.; Kojima, M.; Yoshida, M.; Yamamoto, H.; Westermark, U. Nanostructural assembly of cellulose, hemicellulose, and lignin in the middle layer of secondary wall of ginkgo tracheid. *J. Wood Sci.* **2009**, *55* (6), 409−416.

(2) Capareda, S. C. Pyrolysis. In *Introduction to Biomass Energy Conversions*, Capareda, S. C., Ed.; CRC Press: Boca Raton, 2014; pp 346.

(3) Bridgwater, A. V.; Meier, D.; Radlein, D. An overview of fast pyrolysis of biomass. *Org. Geochem.* **1999**, *30* (12), 1479−1493.

(4) Capareda, S. C. Biomass Liquefaction. In *Introduction to Biomass Energy Conversions*, Capareda, S. C., Ed.; CRC Press: Boca Raton, 2014; pp 439−470.

(5) Behrendt, F.; Neubauer, Y.; Oevermann, M.; Wilmes, B.; Zobel, N. Direct liquefaction of biomass. *Chem. Eng. Technol.* **2008**, *31* (5), 667−677.

(6) Bridgwater, T. Challenges and Opportunities in Fast Pyrolysis of Biomass: Part I Introduction to the technology, feedstocks and science behind a promising source of fuels and chemicals. *Johnson Matthey Technol. Rev.* **2018**, *62* (1), 118−130.

(7) Campanario, F. J.; Gutiérrez Ortiz, F. J. Techno-economic assessment of bio-oil aqueous phase-to-liquids via Fischer−Tropsch synthesis and based on supercritical water reforming. *Energy Convers. Manage.* **2017**, *154*, 591−602.

(8) Evans, R. J.; Milne, T. A. Molecular characterization of the pyrolysis of biomass. 1. Fundamentals. *Energy Fuels* **1987**, *1* (2), 123−137.

(9) Garcia, L.; French, R.; Czernik, S.; Chornet, E. Catalytic steam reforming of bio-oils for the production of hydrogen: effects of catalyst composition. *Appl. Catal., A* **2000**, *201* (2), 225−239.

(10) Bridgwater, T. Challenges and Opportunities in Fast Pyrolysis of Biomass: Part II Upgrading options and promising applications in energy, biofuels and chemicals. *Johnson Matthey Technol. Rev.* **2018**, *62* (2), 150−160.

(11) Vagia, E. C.; Lemonidou, A. A. Thermodynamic analysis of hydrogen production via steam reforming of selected components of aqueous bio-oil fraction. *Int. J. Hydrogen Energy* **2007**, *32* (2), 212−223.

(12) Vagia, E. C.; Lemonidou, A. A. Thermodynamic analysis of hydrogen production via autothermal steam reforming of selected components of aqueous bio-oil fraction. *Int. J. Hydrogen Energy* **2008**, *33* (10), 2489−2500.

(13) Yan, C. F.; Cheng, F. F.; Hu, R. R. Hydrogen production from catalytic steam reforming of bio-oil aqueous fraction over Ni/CeO2-ZrO2 catalysts. *Int. J. Hydrogen Energy* **2010**, *35* (21), 11693−11699.

(14) Bimbela, F.; Oliva, M.; Ruiz, J.; Garcia, L.; Arauzo, J. Hydrogen production via catalytic steam reforming of the aqueous fraction of bio-oil using nickel-based coprecipitated catalysts. *Int. J. Hydrogen Energy* **2013**, *38* (34), 14476−14487.

(15) Medrano, J. A.; Oliva, M.; Ruiz, J.; Garcia, L.; Arauzo, J. Hydrogen from aqueous fraction of biomass pyrolysis liquids by catalytic steam reforming in fluidized bed. *Energy* **2011**, *36* (4), 2215−2224.

(16) Liu, S. M.; Chen, M. Q.; Chu, L.; Yang, Z. L.; Zhu, C. H.; Wang, J.; Chen, M. G. Catalytic steam reforming of bio-oil aqueous fraction for hydrogen production over Ni-Mo supported on modified sepiolite catalysts. *Int. J. Hydrogen Energy* **2013**, *38* (10), 3948−3955.

(17) Gutiérrez Ortiz, F. J.; Campanario, F. J.; Ollero, P. Supercritical water reforming of model compounds of bio-oil aqueous phase: Acetic acid, acetol, butanol and glucose. *Chem. Eng. J.* **2016**, *298*, 243−258.

(18) Sibaja Hernández, B.; Barde, M.; Via, B.; Auad, M. L. Sustainable products from bio-oils. *MRS Bull.* **2017**, *42* (5), 365−370.

(19) Effendi, A.; Gerhauser, H.; Bridgwater, A. V. Production of renewable phenolic resins by thermochemical conversion of biomass: A review. *Renewable Sustainable Energy Rev.* **2008**, *12* (8), 2092−2116.

(20) Barde, M.; Adhikari, S.; Via, B. K.; Auad, M. L. Synthesis and characterization of epoxy Resins from fast pyrolysis bio-oil. *Green Mater.* **2018**, *6* (2), 76−84.

(21) Sibaja, B.; Adhikari, S.; Celikbag, Y.; Via, B.; Auad, M. L. Fast pyrolysis bio-oil as precursor of thermosetting epoxy resins. *Polym. Eng. Sci.* **2018**, *58*, 1296−1307.

(22) Celikbag, Y.; Meadows, S.; Barde, M.; Adhikari, S.; Buschle-Diller, G.; Auad, M. L.; Via, B. K. Synthesis and Characterization of Bio-oil-Based Self-Curing Epoxy Resin. *Ind. Eng. Chem. Res.* **2017**, *56* (33), 9389−9400.

(23) Li, H. W.; Mahmood, N.; Ma, Z.; Zhu, M. Q.; Wang, J. Q.; Zheng, J. L.; Yuan, Z. S.; Wei, Q.; Xu, C. Preparation and characterization of bio-polyol and bio-based flexible polyurethane foams from fast pyrolysis of wheat straw. *Ind. Crops Prod.* **2017**, *103*, 64−72.

(24) Wang, Y. H.; Wu, J. P.; Yu, F.; Chen, P.; Ruan, R. I&EC 62-Preparation of polyurethane foam from microwave pyrolytic bio-oils. *Abstr. Pap. Am. Chem. S.* **2007**, *234*.

(25) Zhou, Z. F.; Xu, W. B.; Fan, J. X.; Ren, F. M.; Xu, C. L. Synthesis and characterization of carboxyl group-containing acrylic resin for powder coatings. *Prog. Org. Coat.* **2008**, *62* (2), 179−182.

(26) Gabriel, S.; Jerome, R.; Jerome, C. Cathodic electrografting of acrylics: From fundamentals to functional coatings. *Prog. Polym. Sci.* **2010**, *35* (1−2), 113−140.

(27) Carretti, E.; Dei, L. G. Physicochemical characterization of acrylic polymeric resins coating porous materials of artistic interest. *Prog. Org. Coat.* **2004**, *49* (3), 282−289.

(28) Ermilova, O. I.; Tyul'kina, I. S.; Kolesova, V. V.; Nikolaev, E. Y. Aqueous-dispersion acrylic adhesives. *Polym. Sci., Ser. C* **2007**, *49* (1), 1−5.

(29) Czech, Z.; Pelech, R. The thermal degradation of acrylic pressure-sensitive adhesives based on butyl acrylate and acrylic acid. *Prog. Org. Coat.* **2009**, *65* (1), 84−87.

(30) Karpushkin, E. A.; Berkovich, A. K.; Sergeyev, V. G. Composites based on acrylic polymers and carbon nanotubes as precursors of carbon materials. *Polym. Sci., Ser. C* **2016**, *58* (1), 85−92.

(31) Venkatesh, A.; Thunberg, J.; Moberg, T.; Klingberg, M.; Hammar, L.; Peterson, A.; Muller, C.; Boldizar, A. Cellulose nanofibril-reinforced composites using aqueous dispersed ethylene-acrylic acid copolymer. *Cellulose* **2018**, *25* (8), 4577−4589.

(32) Wei, C. C.; Xu, Z. Q.; Han, F. H.; Xu, W. K.; Gu, J. J.; Ou, M. R.; Xu, X. P. Preparation and characterization of poly(acrylic acid-co-acrylamide)/montmorillonite composite and its application for methylene blue adsorption. *Colloid Polym. Sci.* **2018**, *296* (4), 653−667.

(33) Liu, X. H.; Yang, R.; Xu, M. C.; Ma, C. H.; Li, W.; Yin, Y.; Huang, Q. T.; Wu, Y. Q.; Li, J.; Liu, S. X. Hydrothermal Synthesis of Cellulose Nanocrystal-Grafted-Acrylic Acid Aerogels with Super-absorbent Properties. *Polymers* **2018**, *10* (10), 1168.

(34) Ha, J.; Kim, M.; Lee, W.; Lee, H.; Han, C.; Koh, W. G.; Ryu, D. Y. Direct measurement of crosslinked surface layer in superabsorbent poly(acrylic acid). *Mater. Lett.* **2018**, *228*, 33−36.

(35) Jong, L.; Liu, Z. Biobased Composites From Crosslinked Soybean Oil and Thermoplastic Polyurethane. *Polym. Eng. Sci.* **2017**, *57* (3), 275−282.

(36) Zhang, C. Q.; Yan, M. G.; Cochran, E. W.; Kessler, M. R. Biorenewable polymers based on acrylated epoxidized soybean oil and methacrylated vanillin. *Mater. Today Commun.* **2015**, *5*, 18−22.

(37) Podkoscielna, B.; Goliszek, M.; Sevastyanova, O. New approach in the application of lignin for the synthesis of hybrid materials. *Pure Appl. Chem.* **2017**, *89* (1), 161−171.

(38) Kim, P.; Weaver, S.; Noh, K.; Labbe, N. Characteristics of Bio-Oils Produced by an Intermediate Semipilot Scale Pyrolysis Auger Reactor Equipped with Multistage Condensers. *Energy Fuels* **2014**, *28* (11), 6966−6973.

(39) ASTM International. Standard Test Method for Water in Crude Oils by Potentiometric Karl Fischer Titration. *ASTM D4377-00(2011)*; ASTM International: West Conshohocken, PA, 2011;

(40) ASTM International. Standard Test Method for Acid Number of Petroleum Products by Potentiometric Titration. *ASTM D664-18e1*; ASTM International: West Conshohocken, PA, 2011;

DOI: 10.1021/acssuschemeng.8b04897
ACS Sustainable Chem. Eng. 2019, 7, 2216−2224

(41) ASTM International. Standard Test Method for Density of Liquid Coatings, Inks, and Related Products. *ASTM D1475-13*; ASTM International: West Conshohocken, PA, 2013; DOI: 10.1520/D1475-13
(42) Ben, H. X.; Ragauskas, A. J. NMR Characterization of Pyrolysis Oils from Kraft Lignin. *Energy Fuels* **2011**, *25* (5), 2322−2332.
(43) Wang, S.; Bassett, A. W.; Wieber, G. V.; Stanzione, J. F.; Epps, T. H. Effect of Methoxy Substituent Position on Thermal Properties and Solvent Resistance of Lignin-Inspired Poly(dimethoxyphenyl methacrylate)s. *ACS Macro Lett.* **2017**, *6* (8), 802−807.
(44) Fleischhaker, F.; Haehnel, A. P.; Misske, A. M.; Blanchot, M.; Haremza, S.; Barner-Kowollik, C. Glass-Transition-, Melting-, and Decomposition Temperatures of Tailored Polyacrylates and Polymethacrylates: General Trends and Structure-Property Relationships. *Macromol. Chem. Phys.* **2014**, *215* (12), 1192−1200.
(45) Rogers, S. S.; Mandelkern, L. Glass formation in polymers. 1. The glass transition of the poly-(n-alkyl methacrylates). *J. Phys. Chem.* **1957**, *61* (7), 985−990.
(46) Oprea, S. Properties of polymer networks prepared by blending polyester urethane acrylate with acrylated epoxidized soybean oil. *J. Mater. Sci.* **2010**, *45* (5), 1315−1320.
(47) Fapeng, W.; Jifu, W.; Chunpeng, W.; Fuxiang, C.; Xiaohuan, L.; Jiuyin, P. Fabrication of soybean protein-acrylate composite miniemulsion toward wood adhesive. *Eur. J. Wood Wood Prod.* **2018**, *76* (1), 305−313.
(48) Barwood, M. J.; Breen, C.; Clegg, F.; Hammond, C. L. The effect of organoclay addition on the properties of an acrylate based, thermally activated shape memory polymer. *Appl. Clay Sci.* **2014**, *102*, 41−50.
(49) Loshaek, S.; Fox, T. G. Cross-linked Polymers. I. Factors influencing the efficiency of cross-linking in copolymers of methyl methacrylate and glycol dimethacrylates. *J. Am. Chem. Soc.* **1953**, *75* (14), 3544−3550.
(50) Loshaek, S. Crosslinked Polymers. II. Glass temperatures of copolymers of methyl methacrylate and glycol dimethacrylates. *J. Polym. Sci.* **1955**, *15* (80), 391−404.
(51) Camacho-Zuniga, C.; Ruiz-Trevino, F. A. A new group contribution scheme to estimate the glass transition temperature for polymers and diluents. *Ind. Eng. Chem. Res.* **2003**, *42* (7), 1530−1534.
(52) Sibaja, B.; Sargent, J.; Auad, M. L. Renewable Thermoset Copolymers from Tung Oil and Natural Terpenes. *J. Appl. Polym. Sci.* **2014**, *131* (23), 7.
(53) Auad, M. L.; Aranguren, M.; Borrajo, J. Epoxy-based divinyl ester resin styrene copolymers: Composition dependence of the mechanical and thermal properties. *J. Appl. Polym. Sci.* **1997**, *66* (6), 1059−1066.
(54) La Scala, J.; Wool, R. P. Property analysis of triglyceride-based thermosets. *Polymer* **2005**, *46* (1), 61−69.

DOI: 10.1021/acssuschemeng.8b04897
ACS Sustainable Chem. Eng. 2019, 7, 2216−2224